A comparison of shimming techniques for optimizing fat suppression in MR mammography

A Comparison of Shimming Techniques for Optimizing Fat Suppression in MR Mammography

Author Names:

Yasuo Takatsu, [1, 2*] Kengo Nishiyama, [1] Tosiaki Miyati, [2] Hideto Miyano, [3] Mariko Kajihara, [4] Thai Akasaka [5]

Author Affiliations:

[1] Department of Radiology, Osaka Red Cross Hospital.

5-30 Fudegasaki, Tennouji-ku, Osaka, 543-8555, Japan.

[2] Division of Health Sciences, Graduate School of Medical Sciences, Kanazawa University.

5-11-80 Kodatsuno, Kanazawa, 920-0942, Japan.

[3] Department of Radiology, Toyonaka Municipal Hospital.

4-14-1 Shibahara-cho, Toyonaka, Osaka, 560-8565, Japan.

[4] Department of Radiology, Kyoto City Hospital.

1-2 Takada-cho, Mibuhigashi, Nakagyo-ku, Kyoto, 604-8845, Japan.

[5] Department of Radiology, Kishiwada City Hospital.

1001 Gakuhara-cho, Kishiwada, Osaka, 596-0822, Japan.

Corresponding Author info:

*Yasuo Takatsu

Department of Radiology, Osaka Red Cross Hospital, 5-30 Fudegasaki, Tennouji-ku, Osaka, 543-8555, Japan.

Tel: +81-6-6774-5111

Fax: +81-6-6774-5131

e-mail: pcblue2@yahoo.co.jp

Abstract

We evaluated the degree of inhomogeneities of fat suppression by using the fully automated three-dimensional breast shimming technique (Image Based-Smart: IB-Smart) and manual setting of a rectangular parallelepiped shim (volume shimming) in MR mammography. Information on breast shape was collected from 9 patients whose images were insufficiently fat-suppressed. A breast phantom made of a thermoplastic sheet was used. Shimming of the magnetic field was done with IB-Smart and various dimensions of volume shims: the anterior to posterior/ right to left/ head to foot directions were set to 75-150/ 150-350/ 50-150 mm. The volumes of inhomogeneously suppressed fat were measured. The calculated volume with inhomogeneous fat suppression with use of IB-Smart was $13.3 \times 10^4 mm^3$. The smallest volume of inhomogeneous fat suppression with volume shimming was $5.4 \times 10^4 mm^3$ when the anterior-posterior/ right-left/ head- foot directions were set to 75/350/50 mm. Our results show that using optimized dimensions of volume shims enables better fat suppression than does IB-Smart.

Key Words: magnetic resonance imaging (MRI); mammography; fat suppression;

homogeneity; shimming; phantom

Introduction

In magnetic resonance imaging (MRI) of the breast, optimized contrast between the tumor and surrounding tissue is vital. Dynamic contrast enhanced magnetic resonance imaging (DCE-MRI) has been shown to be a very useful diagnostic tool in the detection and evaluation of many breast diseases (1–4). The use of fat suppression is recommended for sequences that are used for assessment of contrast enhancement (5). However, optimal fat suppression is strongly dependent on the homogeneity of the main magnetic field (B0), because it influences not only the distribution of the Larmor frequencies of the protons, but also the linearity of the magnetic field gradients required for spatial encoding (6). Therefore techniques such as shimming are necessary for optimization of B0 field uniformity. B0 homogeneity specifically suffers at interfaces between soft tissue and air; this is known as the magnetic susceptibility effect (7, 8). The difference in magnetic susceptibility caused by air around the breast leads to poor B0 homogeneity, and therefore, to inhomogeneous fat suppression.

In general, the breast is structured as an organ protruding from the chest wall. MR mammography is usually done in the prone position (9), and due to the effect of gravity,

the portion between the chest wall and the nipple may occasionally be indented inward. In our study, we called this indentation the “concavity of the breast”. Concavities are created by ptosis and shrinkage of the breast, which are mainly caused by postpartum or menopausal glandular hormonal regression, loss of weight, and other factors that result from aging (10). Concavities lead to inhomogeneous fat suppression and thus may pose a problem for clinical diagnosis.

Optimal fat suppression may be compromised if a fixed frequency offset is used when the shimming or the center frequency is suboptimal. If the optimal frequency offset for fat is determined for the volume of interest, fat suppression can be improved. This procedure is known as volume shimming. A new method, image-based B0 shimming (IBS), has recently been introduced. IBS makes use of the fast field echo image from which the B0 map is constructed. Shim parameters are then calculated for a region of interest (ROI) on the B0 map. In a computer application called IB-Smart, this procedure is fully automated. In IB-Smart, the selection of ROI, which is located over the contours of the breasts in the case of MR mammography, is carried out in the following steps: [1] the outer surface of the breast is outlined by setting of a threshold on the pixel intensity between air and the skin, [2] an algorithm follows the surface of the breast from the approximate position of the nipple to the thorax and arms, and [3] the location of the

lung wall is found by detection of a rapid intensity decrease when going from sternum to lung (11). Although IB-Smart is currently considered one of the most effective methods of fat suppression in MR mammography, fat suppression may still occasionally be inhomogeneous, depending on the shape of the breast.

The “Smart Exam Breast” is a computer application that assists the operator in planning the MR examination by automatically positioning the imaging slices by an automatic recognition algorithm of the breast contour. “Smart Exam Breast” provides consistent fat suppression with IB-Smart. To our knowledge, there have been no previous reports of an application of “Smart Exam Breast” on an experimental breast phantom.

In this study, an experimental breast phantom was created based on data of several patients, from whom the images were insufficiently fat-suppressed. The aim in this study was to evaluate the inhomogeneity of fat suppression by using IB-Smart and volume shimming, and to evaluate how the change in dimensions of the volume shim affects the quality of fat suppression.

Materials and Methods

A 1.5 Tesla MRI scanner with a 7-channel SENSE breast coil (Achieva, Philips

Medical Systems, Best, The Netherlands) was used. The sequence used was a T1-weighted 3D fast field echo sequence (repetition time: 4 ms, echo time: 1.93 ms, flip angle: 10 degrees, field of view: 320x320 mm, matrix: 304x320 [reconstructed matrix: 320], slice thickness: 1 mm, slice gap: 0 mm, number of slices: 100, slice orientation: transverse), with Spectral Attenuated Inversion Recovery (SPAIR) as the fat suppression technique. Two fat suppression techniques with frequency selective inversion pulse - SPAIR and Spectral Presaturation with Inversion Recovery (SPIR) - are available. SPAIR uses an adiabatic radio frequency pulse as a frequency selective inversion pulse at the resonance frequency of fat. Therefore, SPAIR is less sensitive than SPIR to radio frequency (B1) inhomogeneities (12).

The MR images of 40 patients (35 to 92 years old) who underwent MR mammography with IB-Smart were analyzed. We extracted data from 9 patients whose images showed inhomogeneous fat suppression by visual evaluation.

Information on each patient's breast shape, such as the width, length, and depth of the concavity area, was collected from the 9 patients. The widths at the top (the peripheral end of the concavity) (A), the slice with the maximum concavity (B), and the bottom (C) were measured. The distance from the bottom to the nipple was measured. Coronal views at positions A, B, and C and oblique sagittal views at the bottom of each

concavity were created by multiplanar reconstruction (Fig. 1).

The width, length and depth of the concavities were also measured on the reconstructed views. The phantom was designed from the measured values of the deepest and widest concavities in order to be the most susceptible to inhomogeneous fat suppression.

The mold for the phantom was made from paper clay. A previously used thermoplastic sheet for pelvic radiotherapy, MT-HF-1822S (457x559 mm, thickness: 3.2 mm) (MED-TEC), was employed for shaping of the outer shell of the phantom.

The outer shell of the phantom was located on a 7-channel SENSE (Sensitivity Encoding) (13) breast coil. Salad oil (3,300 ml, T_1value: 336.6 ms, T_2value: 106.9 ms) and a mammary gland model (72% Iopamiron 370 + 0.9% NaCl [90 ml], T_1value: 762.2 ms; T_2value: 62.8 ms (14) in an oval plastic case) were installed in the outer shell of the phantom. The accurate center frequency of water was difficult to obtain because the breast phantom was composed mostly of oil and of very little water. In order to resolve this problem, we placed a bottle of copper sulfate (diameter: 6 cm, height: 14.5 cm, demineralized water [1,000 ml] + $CuSO_4$ $5H_2O$ [770 mg] + 2,000 mg NaCl, [250 ml], T_1value: 345.3 ms; T_2value: 319.9 ms) between the two breasts of the phantom and subsequently dismantled it before acquisition of the images. The determination of the central frequency was performed manually.

For evaluation of fat suppression with different methods of shimming, IB-Smart and various dimensions of volume shims were used. The dimensions varied from 75 to 150 mm in the anterior to posterior (AP) direction, 150 to 350 mm in the right to left (RL) direction, and 50 to 150 mm in the head to foot (HF) direction (Fig. 2), and the area where fat was inhomogeneously suppressed was measured by use of Image J, an image analysis software (15).

The measured center frequencies varied among the different dimensions of the volume shims. For relative comparison, however, the center frequency was fixed to that of the largest volume shim (AP/RL/HF direction: 150/350/150 mm) at the time of image acquisition. The difference between the measured center frequency and the fixed value was noted for each case.

The signal intensity of suppressed fat, excluding the mammary gland model, was measured and a histogram was created. A threshold was determined from the histogram by application of a discriminant analysis method. We defined that any pixel with a signal intensity above this threshold value was inhomogeneously fat-suppressed. The total volume of inhomogeneously suppressed fat, excluding the mammary gland model, was measured by summing up of the relevant pixels as voxel data (1x1x1 mm^3/ voxel).

Results

There was a tendency for breasts with inhomogeneous fat suppression to have a clover-like shape on reconstructed coronal views. The maximum length of the concave area was approximately 120 mm, and the maximum depth was 30 mm. The design of the experimental breast phantom was based on these values (Fig. 1).

The “Smart Exam Breast” function was successfully applied to the experimental breast phantom without any errors (Fig. 3a, b). The area with the most inhomogeneous fat suppression was the internal-inferior side of the phantom (Fig. 3b); this tendency closely resembled the patients’ images (Fig. 3c).

In the cases where the lengths of the AP and RL directions of the volume shim were 150/350 mm and 150/250 mm (AP/RL), the center frequency decreased as the volume shim became narrower in the HF direction. On the other hand, in the cases where the lengths of the AP and RL directions were 75/250 mm and 75/150 mm (AP/RL), the center frequency increased as the volume shim became narrower in the HF direction (Fig. 4).

The center frequency of water was set to 63.876845 MHz. The calculated volumes of inhomogeneous suppressed fat are indicated in Fig. 5. The volume was $13.3 \times 10^4 mm^3$

when IB-Smart was used. The smallest volume with volume shimming was $5.4x10^4$ mm^3, in which case the dimensions were 75/350/50 mm in the AP/RL/HF directions (Figs. 5, 6).

When the length in the AP direction was 75 mm, there was a tendency for inhomogeneously suppressed fat to be seen near the abdominal wall, especially when the length in the HF direction was 50 mm (Fig. 6). The homogeneity of fat suppression on the lateral edges deteriorated when the size of the volume shim was reduced in the RL direction (Fig. 7).

Discussion

In MR mammography, the magnetic field tends to be inhomogeneous because of the breasts' characteristic shape that has a large surface area in contact with air. It is likely that concavities further increase the area that is in contact with air, and therefore cause the quality of fat suppression to deteriorate. The center frequency almost always differs according to the dimensions of the volume shim, and therefore the homogeneity of fat suppression may vary. Both the center frequency and the dimension of the volume shim are parameters that affect the homogeneity of fat suppression. In clinical practice, the actual center frequency is adjusted according to the dimension of the volume shim or

after application of IB-Smart. The reason we fixed the center frequency in all cases is because we attempted to disclose a relative relationship between the dimension of the volume shim and the homogeneity of fat suppression. As a result, the difference in the center frequency between each case and that of the largest volume shim did not necessary correlate with the volume of inhomogeneous suppressed fat. Therefore, we believe that, in our results, the dimensions of the volume shim are the main contributing factor to the quality of fat suppression. If the center frequency is optimized for each case, as is the case in clinical practice, further improvement of fat suppression is likely to be accomplished.

The "Smart Exam Breast" function was applied successfully to the experimental breast phantom, which indicated the validity of the phantom for this study.

It is important to consider the material used for the phantom. The thermoplastic sheet used for pelvic radiotherapy allows for high flexibility of shape, has convenient lightness and hardness, and can reduce the cost of the experiment.

It is quite possible that this method of building an experimental breast phantom can be utilized in other studies, such as optimization of pulse sequences or contrast measurements of tumor and mammary glands, by inclusion of a tumor model in the phantom.

Another approach to achieving fat suppression is the Dixon technique, where in-phase and opposite-phase images acquired at two different echo times are combined to produce separate water and fat images (16). The Dixon technique has been applied to DCE-MRI at 1.5 T and has been shown to provide better fat suppression results than are obtained with conventional fat-suppression techniques (17). Moreover, the improved Dixon technique has been reported to reduce the effective acquisition time for each temporal frame without sacrificing the signal-to-noise ratio (18). However, the Dixon technique may not be available for all MRI scanners.

The breast morphology varies from person to person. Pre-menopausal women tend to have more glandular tissue and post-menopausal women have more fat. One of the limitations of our study is that the quality of fat suppression according to the degree of mammary fat was not assessed. The next step will be to create diverse forms of phantoms to elucidate a more precise correlation between various forms of concavities and fat suppression effects.

Our results show that, although IB-Smart is vulnerable to magnetic field inhomogeneities, it could be improved by narrowing of the volume shim in the HF direction.

Conclusion

In MR mammography, fat suppression tends to be inhomogeneous in breasts with concavities. Our study suggests that use of optimized volume shims enables better fat suppression than does IB-Smart in such cases.

Acknowledgments

The author would like to thank Yoshinori Hirose and Tsuneyuki Tomita from the radiotherapy division of the department of radiology at the Osaka Red Cross Hospital for the construction of the phantom.

The authors declare that they have no conflict of interest.

References

1. Kuhl C. The current status of breast MR imaging. Part I. Choice of technique, image interpretation, diagnostic accuracy, and transfer to clinical practice. Radiology. 2007;244:356–378.

2. Kuhl CK. Current status of breast MR imaging. Part 2. Clinical applications. Radiology. 2007;244:672–691.

3. Turnbull LW. Dynamic contrast-enhanced MRI in the diagnosis and management of breast cancer. NMR Biomed. 2009;22:28–39.

4. Krause U, Kroencke T, Spielhaupter E, et al. Contrast-enhanced magnetic resonance angiography of the lower extremities: standard-dose vs. high-dose gadodiamide injection. J Magn Reson Imaging. 2005;21:449–454.

5. American College of Radiology. ACR practice guideline for the performance of magnetic resonance imaging (MRI) of the breast. American College of Radiology. 2008;25:1-7

6. Dietrich O, Reiser MF, Schoenberg SO. Artifacts in 3-T MRI: Physical background and reduction strategies. Eur J Radiol. 2008;65:29–35.

7. Schenck JF. The role of magnetic susceptibility in magnetic resonance imaging: MRI magnetic compatibility of the first and second kinds. Med

Phys.1996;23:815-850.

8. Penner RR, Hargreaves B, Glover G, et al. Breast MRI at 3T. Appl Radiol. 2009;6-13.
9. Mann RM, Kuhl CK, Kinkel K, et al. Breast MRI: guidelines from the European Society of Breast Imaging. Eur Radiol. 2008;18:1307-1318.
10. Regnault P. Breast Ptosis Definition and Treatment. Clin Plast Surg. 1976;3(2):193-203.
11. Simonetti AW, Holthuizen R, Harder CJ, et al. 3D breast segmentation for image based shimming. Proc Intl Soc Magn Reson Med. 2009;17:2114.
12. Petra M, Carsten K, Frank T, et al. Diffusion-weighted whole-body MR imaging with background body signal suppression: a feasibility study at 3.0 Tesla. Eur Radiol. 2007; 17: 3031–3037.
13. Klaas PP, MarkusW, Markus B, et al. SENSE: Sensitivity Encoding for Fast MRI. Magn Reson Med. 1999; 42: 952–962.
14. Mazzara GP, Briggs RW, Wu Z, et al. Use of modified polysaccharide gel in developing a realistic breast phantom for MRI. Magn Reson Imaging. 1996;14(6): 639-648.
15. Abramoff MD, Magalhaes PJ, Ram SJ. Image Processing with ImageJ.

Biophotonics International. 2004;11(7):36-42.

16. Dixon WT. Simple proton spectroscopic imaging. Radiology. 1984;153:189–194.
17. Le-Petross H, Kundra V, Szklaruk J, et al. Fast three-dimensional dual echo Dixon technique improves fat suppression in breast MRI. J Magn Reson Imaging. 2010; 31:889–894.
18. Le Y, Kroeker R, Kipfer HD, et al. Development and Evaluation of TWIST Dixon for Dynamic Contrast-Enhanced (DCE) MRI With Improved Acquisition Efficiency and Fat Suppression. J Magn Reson Imaging. 2012;36:483–491.

Fig. 1

Blueprint of the phantom

Making a multiplanar reconstruction of the coronal view (A, B, C) from a transverse view (original).

Fig. 2

Setting the dimensions of the volume shim

The dimensions of the volume shim were varied: 50 to 150 mm (HF direction), 150 to 350 mm (RL direction), 75 and 150 mm (AP direction).

Fig. 3

Images of the phantom and human breast

(a) Outer shell of the phantom made of a radiotherapy shell.

The inhomogeneously fat-suppressed area of the left breast in the phantom image (b) resembles that in the human breast image (c) . Both coronal images (b, c) were reconstructed from the set of the transverse images obtained with “Smart Exam Breast”.

Fig. 4

Center frequency in every case

The dotted line indicates the center frequency of the largest volume shim.

Fig. 5

Volumes of inhomogeneously suppressed fat for each shim

The dimensions of the shim with the smallest volume were 75/350/50 mm (AP/RL/HF)

Fig. 6

Maximum Intensity Projection (MIP) images of the phantom

Both HF and AP directional MIP images were reconstructed from the set of transverse images obtained with IB-Smart (a) or volume shim: 150/350/50 mm (b), 75/350/50 mm (AP/RL/HF) (c).

Fig.7

MIP images of the phantom of the right breast

The homogeneity of fat suppression of the lateral edges was worse (white arrow) when the volume shim was narrowed in the RL direction.

Volume shim: 150/150/50 mm (a), 150/250/50 mm (b), 150/350/50 mm (c)

(AP/RL/HF)

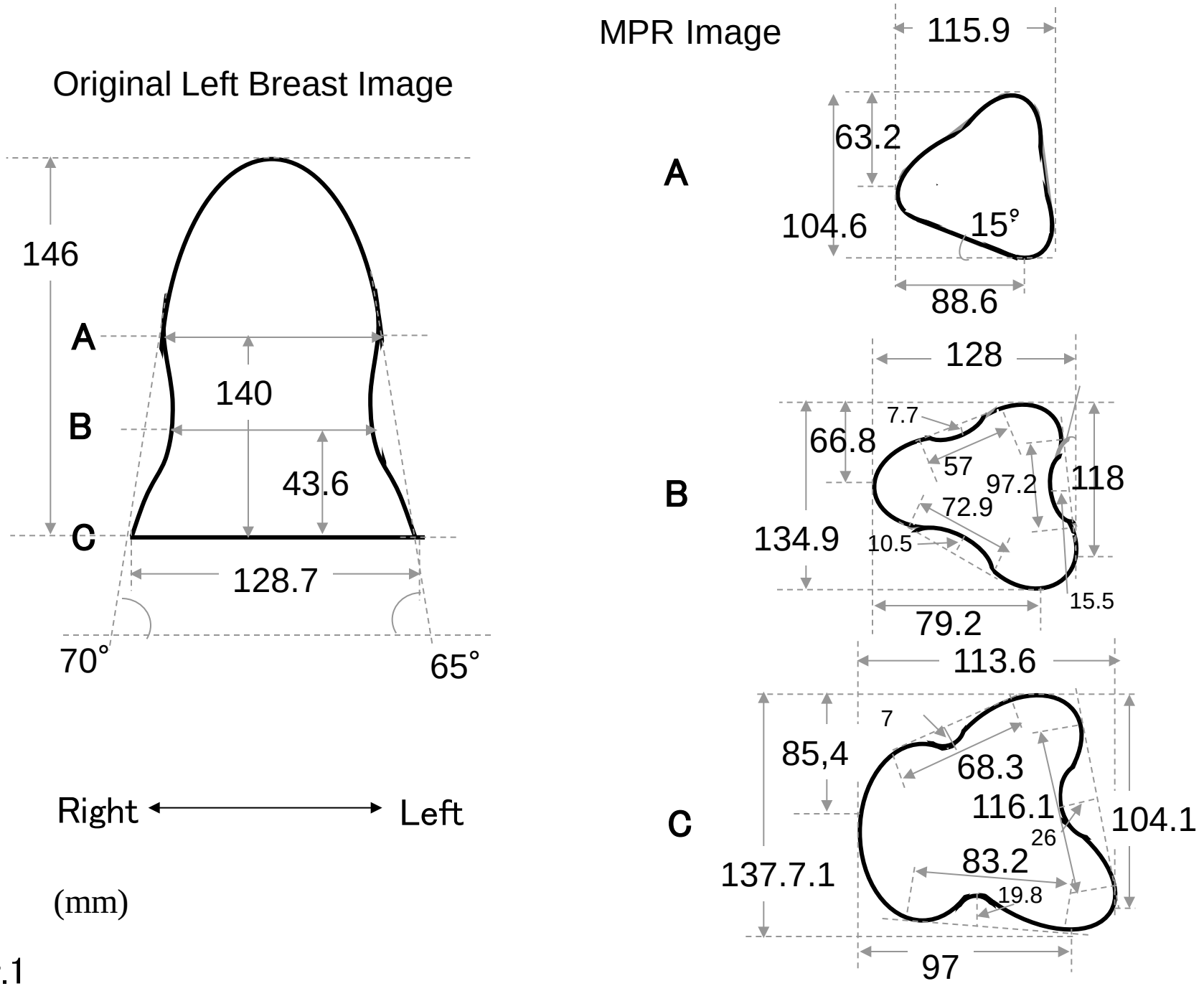
Original Left Breast Image
146
A
B
C
140
43.6
128.7
70°
65°
Right
Left
(mm)
MPR Image
115.9
63.2
104.6
15°
88.6
A
128
66.8
7.7
57
97.2
118
72.9
134.9
10.5
15.5
79.2
B
113.6
85,4
7
68.3
116.1
104.1
26
83.2
137.7.1
19.8
97
C

Fig.1

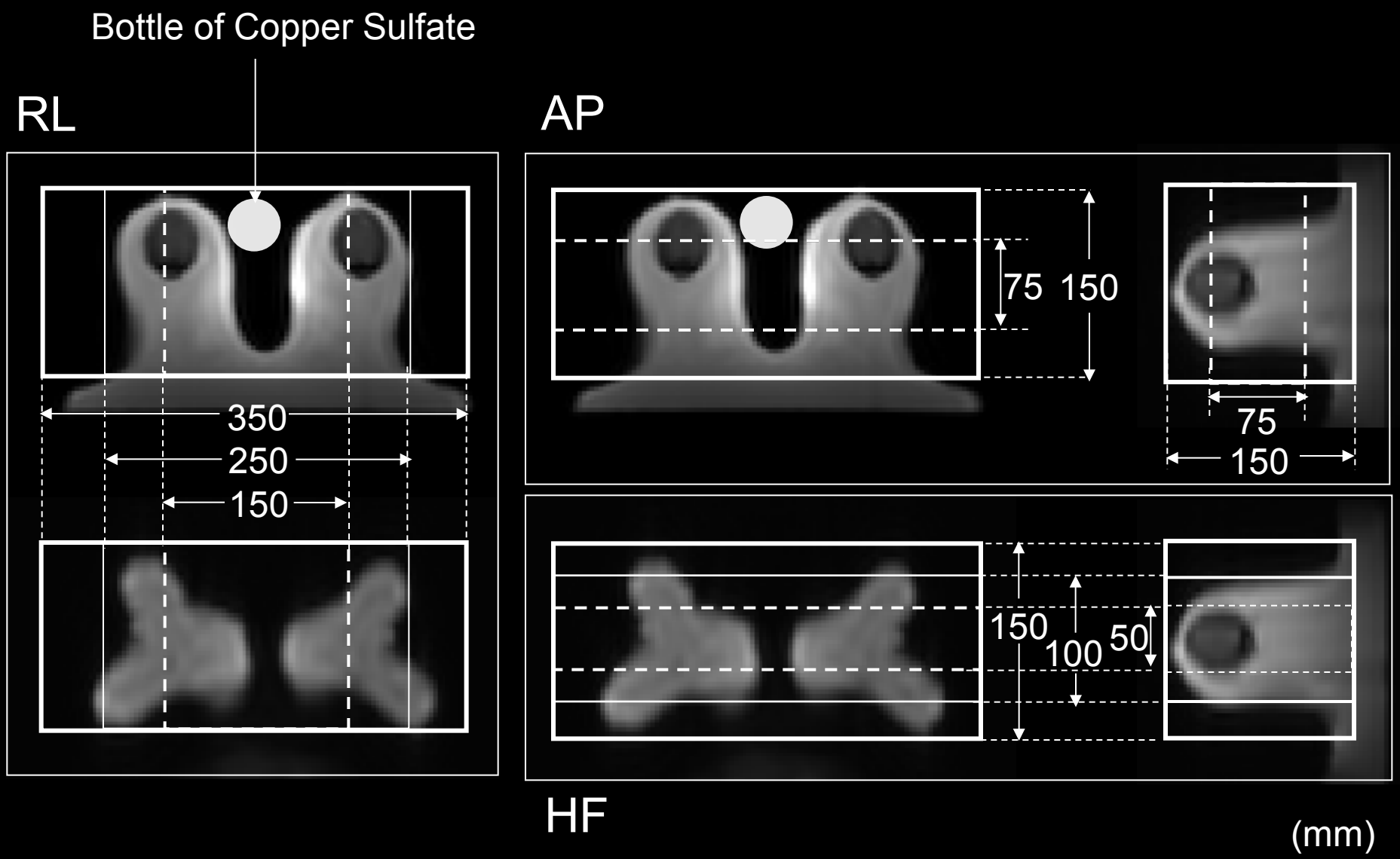
Bottle of Copper Sulfate
RL
AP
350
250
150
75
150
75
150
150
100
50
HF
(mm)

Fig.2

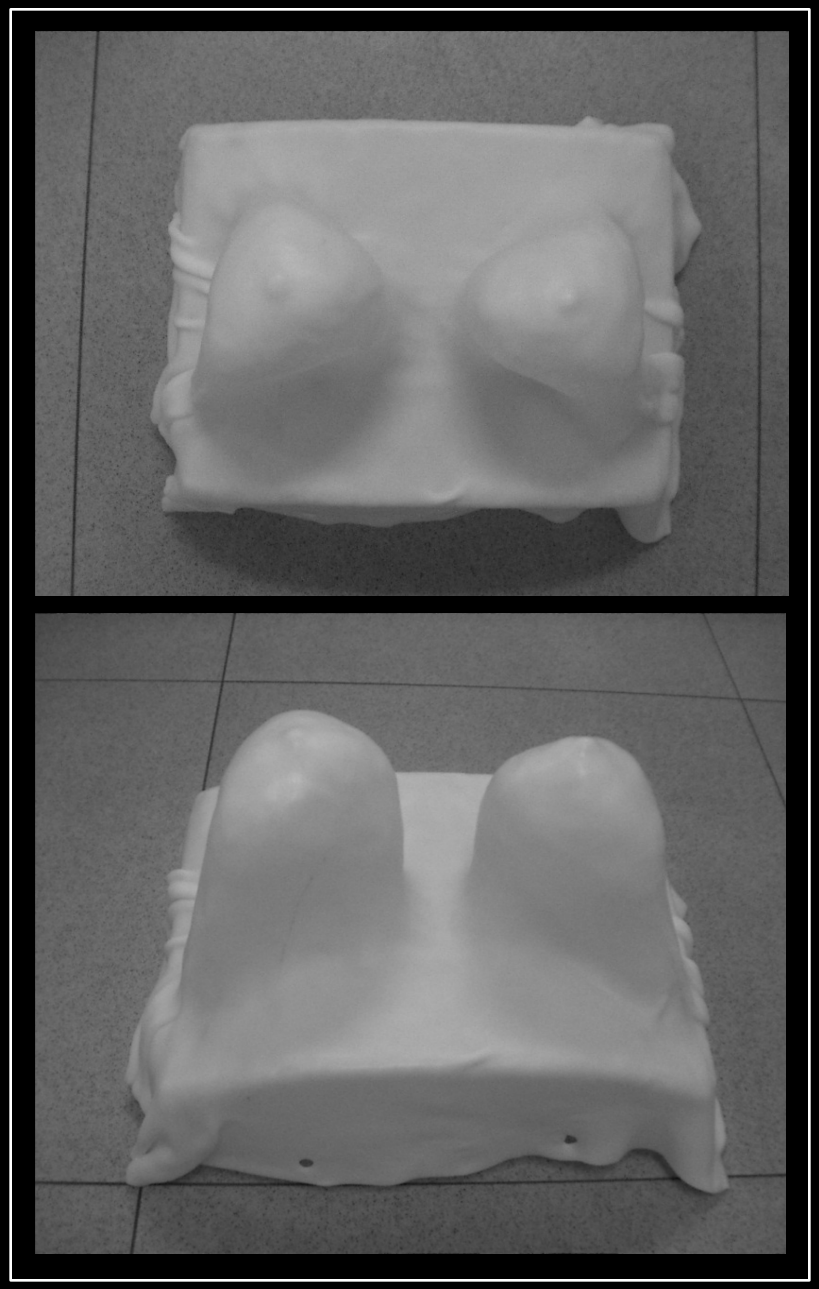

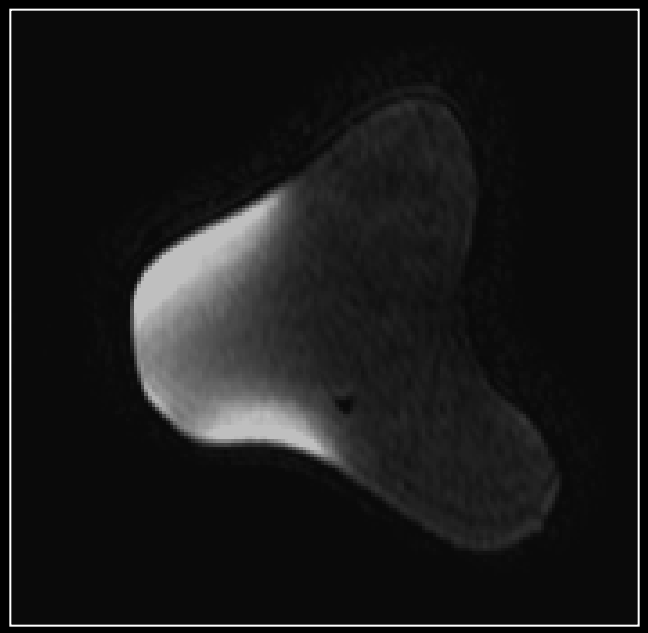

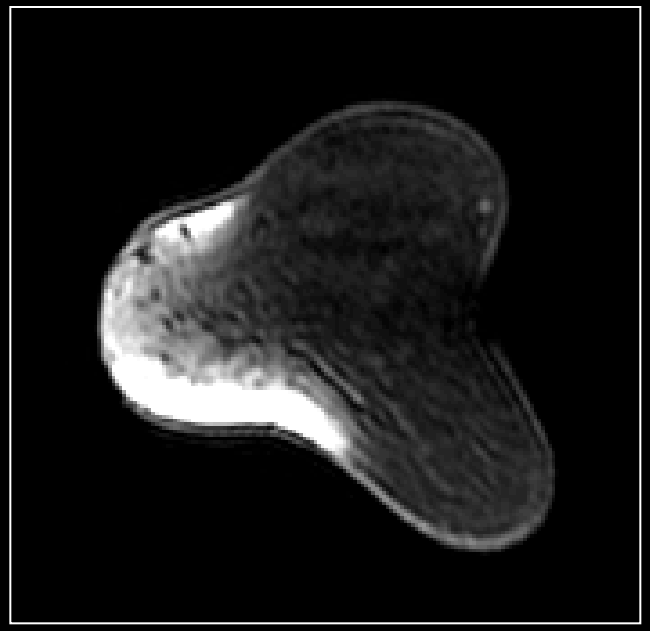

Fig.3

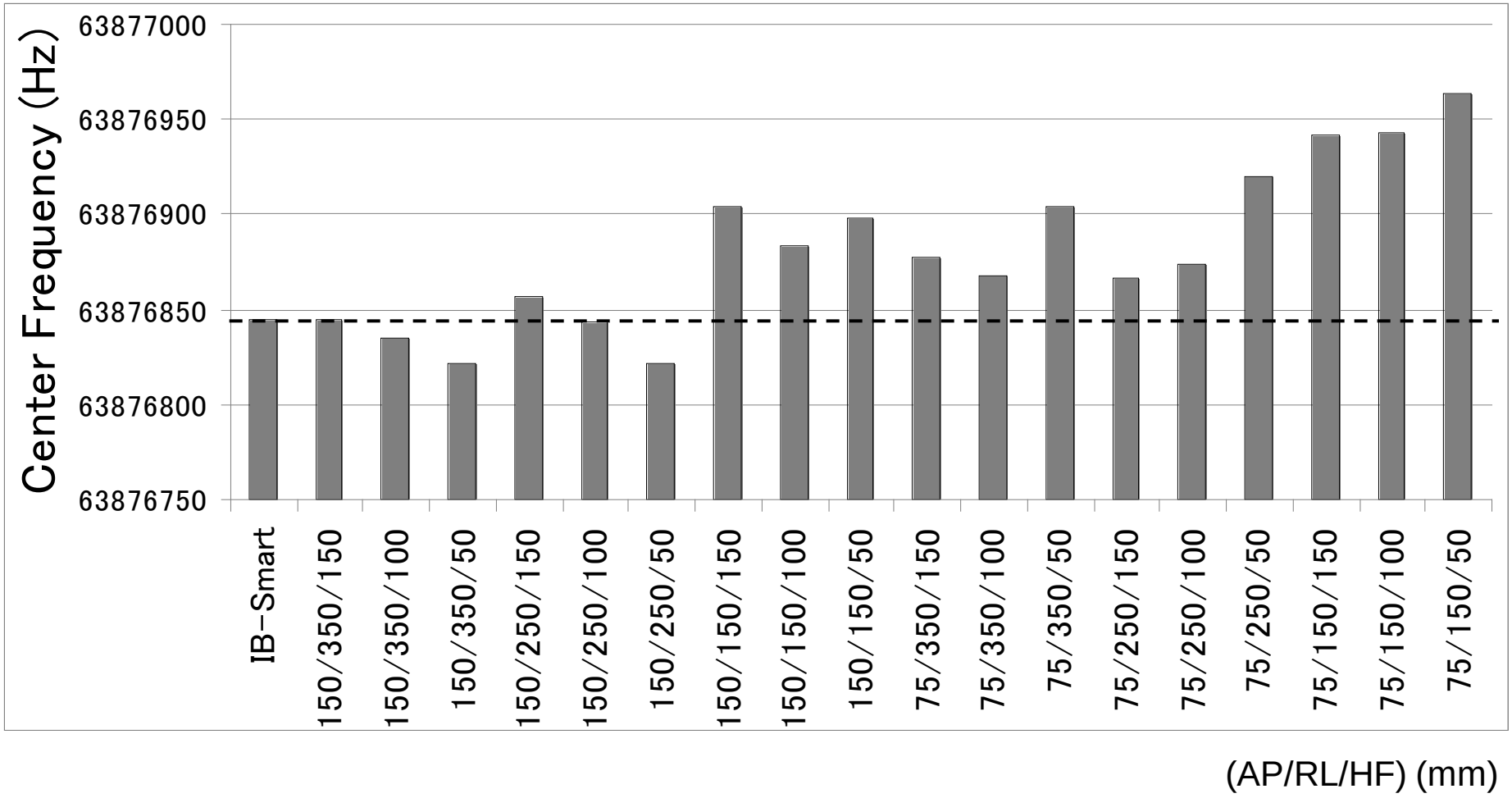
Center Frequency (Hz)
63877000
63876950
63876900
63876850
63876800
63876750
IB-Smart
150/350/150
150/350/100
150/350/50
150/250/150
150/250/100
150/250/50
150/150/150
150/150/100
150/150/50
75/350/150
75/350/100
75/350/50
75/250/150
75/250/100
75/250/50
75/150/150
75/150/100
75/150/50
(AP/RL/HF) (mm)

Fig.4

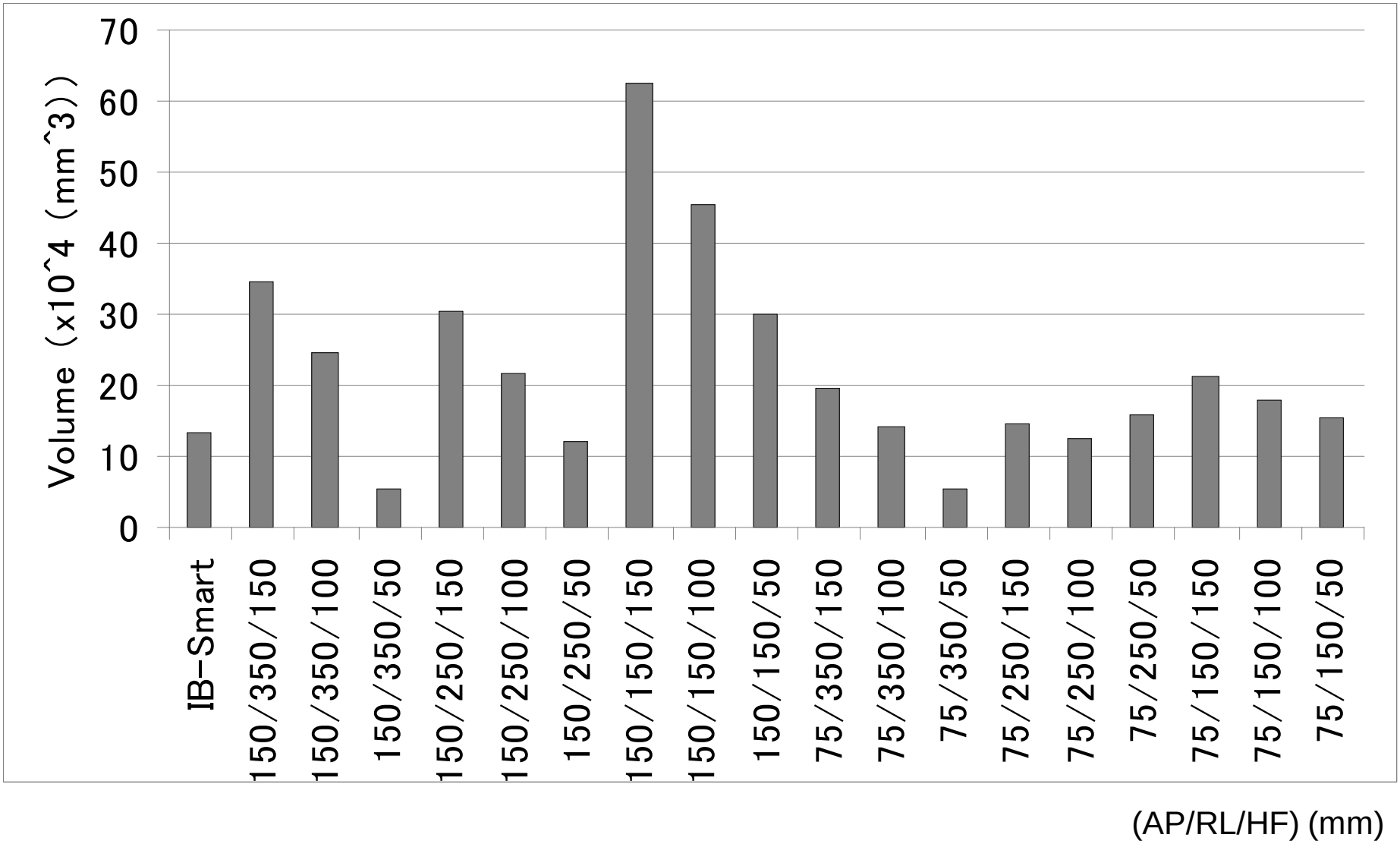
Volume (x10^4 (mm^3))
70
60
50
40
30
20
10
0
IB-Smart
150/350/150
150/350/100
150/350/50
150/250/150
150/250/100
150/250/50
150/150/150
150/150/100
150/150/50
75/350/150
75/350/100
75/350/50
75/250/150
75/250/100
75/250/50
75/150/150
75/150/100
75/150/50
(AP/RL/HF) (mm)

Fig.5

MIP of HF Direction

MIP of AP Direction

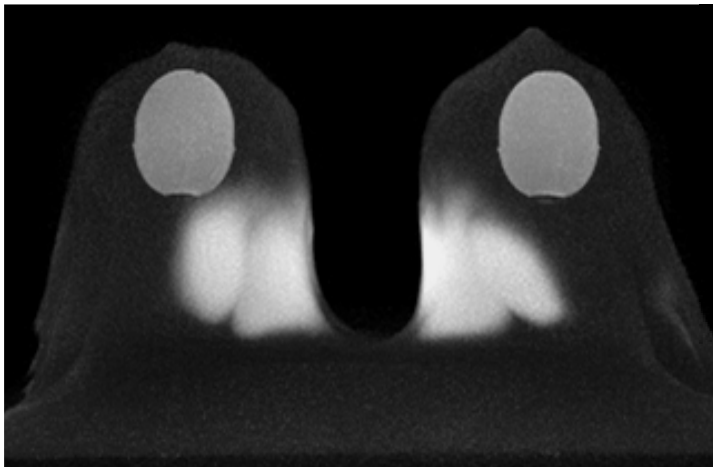

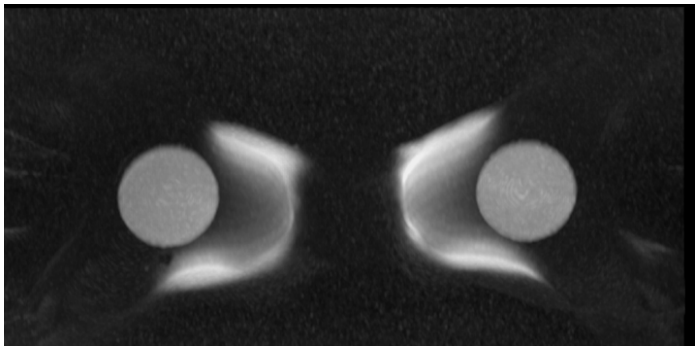

IB-smart

a

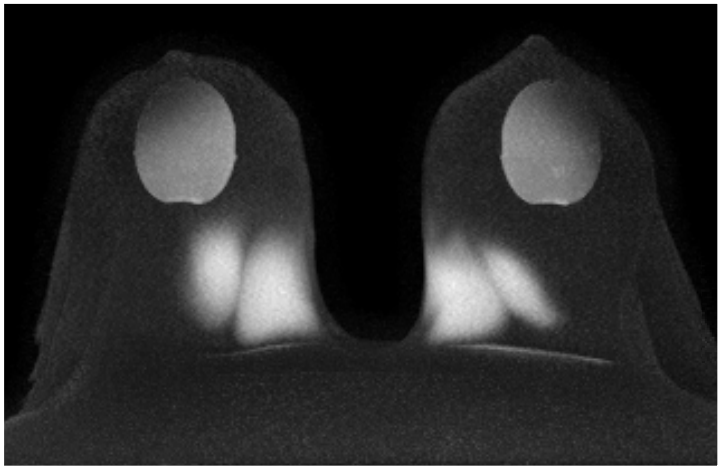

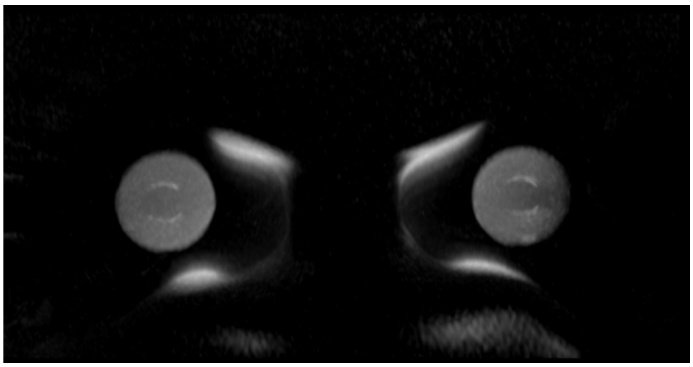

150/350/50

b

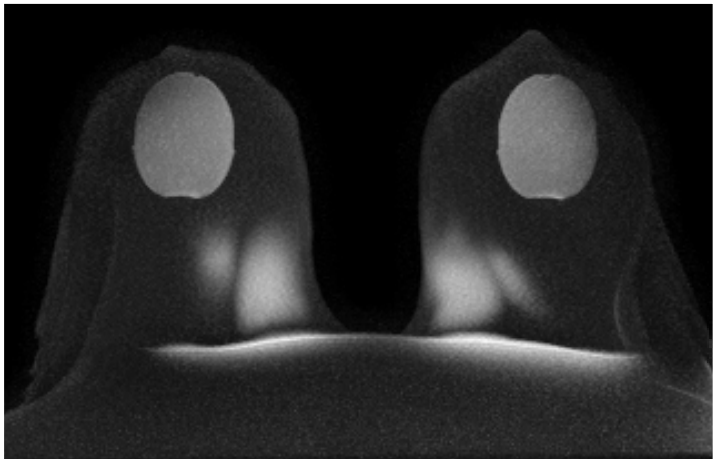

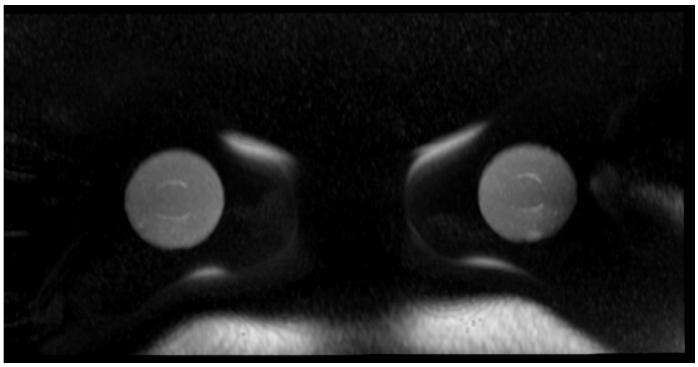

75/350/50

c

(AP/RL/HF) (mm)

Fig.6

Fig.7

(AP/RL/HF)

(mm)